Photodynamics in Cl_2-Doped Xenon under High Pressures: A Diamond Anvil Cell Study

Allen I. Katz and V. A. Apkarian*

Department of Chemistry, University of California, Irvine, California 92717 *(Received: February 13, 1990)*

High-pressure studies of molecular dissociation, atomic mobility, diffusion, and recombination photodynamics are reported for chlorine-doped solid xenon contained in a diamond anvil cell. The photogeneration of atoms is monitored by following emission from Xe_2Cl, the emission spectra and relaxation dynamics of which are characterized as a function of pressure and temperature. At 308 nm, the direct dissociation of Cl_2 via its $^1\Pi_u \leftarrow X$ dissociative absorption is prohibited at all studied pressures (2–10 GPa) and temperatures (30–300 K). Instead, dissociation via the two-photon-induced harpoon process: $Xe + Cl_2 + 2h\nu \rightarrow [Xe^+Cl_2^-] \rightarrow Cl + Xe^+Cl^-$, is observed. The cross section of the latter process, at 2 GPa, is large and shows a strong temperature dependence—10^{-44} cm^4 s at 300 K, 10^{-47} cm^4 s at 40 K. At room temperature and pressures above 5 GPa, atomic Cl is stable with respect to recombination for periods of many weeks, implying a diffusion constant less than 10^{-20} cm^2 s^{-1}. Recombination at 2 GPa proceeds over the period of several hours. The radiative dissociation of Xe_2Cl leads to atomic mobility and subsequent diffusion-controlled recombination. The extent of dissociation is controlled by the competition between rates of photogeneration and photomobility driven recombination.

Introduction

The photodynamics of impurities isolated in crystalline rare gas solids constitute simple prototypes of condensed-phase reactive dynamics. Charge transfer, photodissociation, radiative dissociation, diffusion, and recombination are among the phenomena that can be conveniently scrutinized in such solids. Studies of these systems have in the past been limited to a narrow range of experimental conditions: cryogenic temperatures and high vacuum. These limitations can be eliminated and a much broader range of physical conditions can be accessed by resorting to high pressures. Indeed, the pressures necessary to maintain rare gases as solids at room temperature are quite modest—4.8, 1.2, 0.8, and 0.4 GPa for Ne, Ar, Kr, and Xe, respectively[1]—on the scale of pressures attainable by present day diamond anvil cell (DAC) designs.[2] Experimental studies in such an expanded temperature window, along with the added dimension of density control in these compressible solids, allows for a significantly more rigorous test of our understanding of these systems by critical comparisons with theory. To our knowledge, with this paper we report the first use of a diamond anvil cell for such photodynamical studies.

Xenon-doped with molecular chlorine was the system chosen for these studies. Our main intention was the characterization of the solid-state photodissociation dynamics of molecular chlorine. The photodissociation of molecular halogens in rare gas solids, and Cl_2 in particular, remains the subject of both experimental and theoretical investigations. The earliest experimental studies in this system are due to Bondybey and co-workers, who showed that, in cryogenic Ar and Kr matrices, the photodissociation of Cl_2 was prohibited by a nearly perfect cage effect.[3] It was later demonstrated that, while direct dissociation via the repulsive $^1\Pi_u$ surface of Cl_2 is inhibited in such matrices, dissociation via ionic charge transfer potentials is efficient.[4] The efficiency of these photoinduced harpoon processes could be attributed to cooperative dynamics between the guest molecule and its immediate cage, and a major role was ascribed to charge delocalization in the solid.[5,6] Very recent experimental studies, using synchrotron radiation, have shown that direct dissociation of the molecule can be effected in all rare gases when irradiated in the deep UV region, for dissociation excess energies greater than 4 eV.[7] Experimental characterization of this seemingly simple system is far from complete.

Molecular dynamics (MD) simulations of Cl_2 photodissociation in solid xenon were reported very recently.[8] According to these simulations, the absence of dissociation at cryogenic temperatures (at dissociation excess energies of 1.3 eV) in solid xenon is due to an unfavorable alignment of the molecule in its trap site. Accordingly, a thermal threshold for dissociation at 90 K is observed, which coincides with the onset of nearly free rotation of the molecule in the simulations. A rather intriguing prediction of the MD studies was the nonmonotonic temperature dependence of photodissociation quantum yields. The cage exit probability of fragments shows a minimum near 125 K, presumably due to a dynamic cage effect. Similar predictions, with respect to temperature dependence, have also been made for the photodissociation of HI in crystal Xe.[9] Under standard conditions, the theoretical predictions in the case of Cl_2/Xe are difficult to verify experimentally. At the elevated temperatures of the predictions, solids maintained under vacuum sublime. While high temperature inclusion crystals of Xe can be prepared under equilibrium pressure in cryocells, at temperatures above ~110 K, due to the onset of self-diffusion, clustering of impurities prevents studies of the isolated species. Resorting to high pressures overcomes these difficulties and affords meaningful comparisons with theory. Furthermore, it is worth noting that, due to the compressibility of rare gases, under high pressures it is possible to attain densities at which even the equilibrium properties of the solids sample the many-body terms of interaction potentials. Hence, the main input in theoretical simulations of dynamical processes, namely the interaction potentials, can in principle be most rigorously tested.

There are obvious experimental difficulties and limitations associated with photodynamical studies in DAC's. The optical transmission of diamonds is fairly limited in the UV region, and the microscopic sample sizes used in such studies decree that the detection technique be sensitive. In the absence of direct means for structural characterization, it is also important to have a firm understanding of the effects of temperature and pressure cycling on the sample under study. Thus, in addition to the fundamental motivations, the selection of the system for investigation in the present studies had the above experimental considerations in mind. The first dissociative absorption continuum of Cl_2, the $^1\Pi_u \leftarrow X$ ($^1\Sigma_g$) band, peaks near 330 nm—a spectral range in which the transmission of the anvil diamonds is adequate for excitation of the sample. Photodissociation of Cl_2 in xenon can be conveniently studied by monitoring the generation of Cl atoms in the solid. The

(1) Lohr, P. H.; Eversole, W. G. *J. Chem. Eng. Data* **1962**, *7*, 42. Grace, J. D.; Kennedy, G. C. *J. Phys. Chem. Solids* **1967**, *28*, 977. Crawford, R. K.; Daniels, W. B. *J. Chem. Phys.* **1971**, *55*, 5651.
(2) For a DAC review see: Jayaraman, A. *Rev. Sci. Instrum.* **1986**, *57*, 1013.
(3) Bondybey, V. E.; Fletcher, C. *J. Chem. Phys.* **1976**, *64*, 3615. Bondybey, V. E.; Brus, L. E. *J. Chem. Phys.* **1975**, *65*, 620; **1976**, *64*, 3724.
(4) Fajardo, M. E.; Apkarian, V. A. *J. Chem. Phys.* **1986**, *85*, 5660.
(5) Fajardo, M. E.; Apkarian, V. A. *Chem. Phys. Lett.* **1987**, *134*, 51.
(6) Gerber, R. B.; Alimi, R.; Apkarian, V. A. *Chem. Phys. Lett.* **1989**, *158*, 257.
(7) Schwentner, N. Private communications.
(8) Alimi, R.; Brokman, A.; Gerber, R. B. *J. Chem. Phys.* **1989**, *91*, 1611.
(9) Alimi, R.; Gerber, R. B.; Apkarian, V. A. *J. Chem. Phys.* **1988**, *89*, 174.

0022-3654/90/2094-6671$02.50/0

latter is achieved by monitoring the Xe_2Cl radiative relaxation upon charge-transfer excitation of Cl/Xe—a laser induced fluorescence technique of demonstrated sensitivity.[10] Finally, rare gas solids have been the subject of extensive DAC studies.[11] It is known from such studies that, under pressure, the solids crystallize and yield relatively sharp diffraction patterns; and reliable equations of state for the rare gases, Xe in particular, have been obtained from such studies.[12]

As will be discussed in the main body of this paper, several unanticipated results have emerged from our studies. Of these, we note here that we have failed to observe direct photodissociation of Cl_2 even at room temperature; in lieu we observe dissociation via the two-photon-induced harpoon process.[13] A characterization of this process, photomobility of Cl atoms upon radiative dissociation of charge-transfer complexes, diffusion, and atomic recombination as a function of temperature and pressure of the solid are the subjects of this paper.

Experimental Section

A diamond anvil cell, of the Merrill–Bassett design,[14] was constructed out of Be–Cu for these studies. Type IIa diamonds, selected for low fluorescence, were used. Inconel sheet (inconel X718), prepressed to 70 μm, was used as the sealing gasket. A closed-cycle cryostat was retrofitted to accommodate the cell, and to enable sample deposition and closure of the cold cell under vacuum. This was achieved by bolting the cell back plate to the cryo-tip, while the front plate was maintained at a distance of 5–10 mm on guide pins. The space between plates was sufficient to accommodate a 1/16-in retractable stainless steel tube, through which the premixed gas sample could be deposited on the cold diamond surface. After deposition of the sample, the cell could be shut and pressurized under vacuum by three bolt drivers introduced through double O-ring seals on the shroud. Throughout this operation, the cell temperature remained below 40 K. Temperature was monitored by a gold–chromel thermocouple anchored on the cell body. The pressure in the DAC was determined by the shift in ruby lines.[15] Ruby filings were introduced in the cell prior to sample deposition for this purpose. The clear aperture of the gasket, after pressurization of the DAC, was determined under a microscope to be ~250 μm, while the spacing between the diamonds was estimated to be ~50 μm.

Most of the studies to be reported here were carried out using a XeCl excimer laser (Lambda Physik, EMG 201) operating at 308 nm. The transmission of the diamond at this wavelength was 55% (~20% due to reflection losses, and the rest due to impurity absorptions). Excitation of the diamond at 308 nm produces a broad emission centered at ~470 nm, which is ascribed to defect luminescence.[16] In the pressure range of the present studies, and given the large difference between compressibilities of the sample and diamond, the strength of the diamond emission can safely be assumed to remain independent of cell pressure. This emission is used to advantage as an internal standard for the calibration of sample emission intensities. The optical damage threshold of the diamond at 540 nm was determined to be near 130 MW cm^{-2}. The damage threshold at 308 nm is expected to be lower due to greater absorption. The laser fluence in the experiments was kept nearly 2 orders of magnitude below the threshold. A 30 cm focal length lens is used to bring the laser beam to focus ~3 cm before the cell. The emission from the cell was collected through a 0.3-m monochromator (McPherson 218) and detected with a thermoelectrically cooled photomultiplier (Hamamatsu R943-02). The ruby fluorescence was recorded by a photon counter (SRS SR400), while the shorter lived emissions from the exciplex and diamond impurities were recorded with a 500-MHz digitizing/averaging scope (Tektronix 2440).

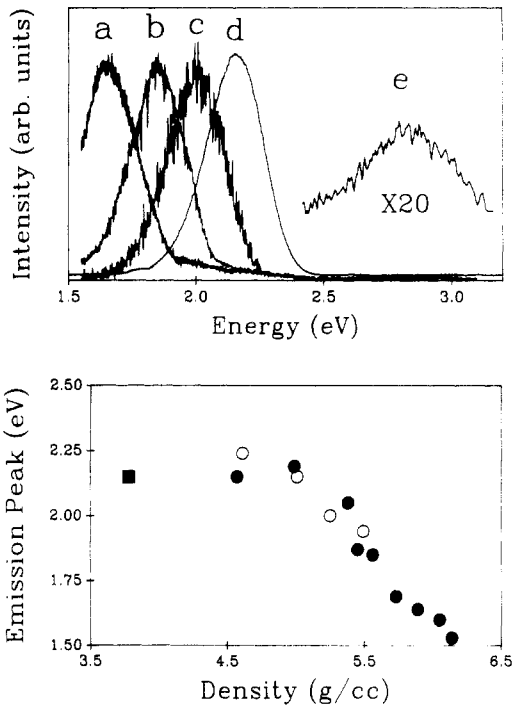

Figure 1. Pressure (density) dependence of Xe_2Cl emission. In the top panel spectra obtained from the DAC under different pressures and temperatures are shown: (a) 8.0 GPa, 30 K; (b) 5.8 GPa, 30 K; (c) 4.2 GPa, 298 K. The 12 K matrix (zero pressure) emission spectrum is also shown (d); and the diamond fluorescence is shown on an expanded ordinate in trace (e). All of the spectra were obtained by 308-nm excitation and after dispersion through a 0.3-m monochromator. In the lower panel, the emission band maxima are plotted as a function of sample density: filled circles, 30K data; open circles, 298 K data; filled square, zero pressure, 12 K matrix spectrum.

All of the experiments to be reported here were from a single sample of original composition 1:500 Cl_2:Xe. The sample was prepared in a glass manifold, using Cl_2 of 99% and Xe of 99.9995% purity. The premixed gas was deposited at 20 K, and its presence on the diamond anvils was verified visually by observation of the yellow Xe_2Cl emission upon 308-nm irradiation. Thus, the molecular chlorine was at least partially dissociated prior to sealing of the cell. The same sample was studied over a period of approximately 9 months.

Results

Emission spectra obtained after extensive irradiation of the 1:500 Cl_2:Xe sample at 308 nm, soon after sealing of the cell, are shown in Figure 1a. Also shown in the same figure are a spectrum of Xe_2Cl obtained from a 12 K Xe matrix at zero pressure and a sample diamond emission. Although a large spectral shift is observed as a function of pressure, the spectra maintain their broad profiles with fwhm of 2200 cm^{-1} independent of pressure. The emission maxima as function of density are plotted in Figure 1b. Data taken at a variety of temperatures ranging from 20 to 298 K are included in the figure. The emission band shape and position are insensitive to temperature. Note that the spectral shift as a function of density shows a linear dependence after an initial flat region.

The exciplex fluorescence from the cell is observed to decay exponentially. The time evolution of fluorescence and a single exponential fit to it are shown in Figure 2. The density dependence of the fluorescence relaxation rates, measured at several different temperatures, is illustrated in Figure 2. At high pressures,

(10) Lawrence, W. G.; Apkarian, V. A. *Isr. J. Chem.* **1990**, *30*, 135.
(11) Most recently see; Hemley, R. J.; Zha, C. S.; Jephcoat, A. P.; Mao, H. K.; Finger, L. W.; Cox, D. E. *Phys. Rev. B* **1989**, *39*, 11820. Goettel, K. A.; Eggert, J. H.; Silvera, I. F.; Moss, W. C. *Phys. Rev. Lett.* **1989**, *62*, 665. Reichlin, R.; Brister, K. F.; McMahan, A. K.; Ross, M.; Martin, S.; Vohra, Y. K.; Ruoff, A. L. *Phys. Rev. Lett.* **1989**, *62*, 669. Polian, A.; Itie, J. P.; Dartyge, D.; Fontaine, A.; Tourillon, G. *Phys. Rev. B* **1989**, *39*, 3369.
(12) Syassen, K.; Holzapfel, W. B. *Phys. Rev. B* **1978**, *18*, 5826. Zisman, A. N.; Aleksandrov, I. V.; Stishov, S. M. *Phys. Rev. B* **1985**, *32*, 484.
(13) Fajardo, M. E.; Withnall, R.; Feld, J.; Okada, F.; Lawrence, W.; Wiedeman, L.; Apkarian, V. A. *Laser Chem.* **1988**, *9*, 1.
(14) Merrill, L.; Bassett, W. A. *Rev. Sci. Instrum.* **1974**, *45*, 290.
(15) Barnett, J. D.; Block, S.; Piermarini, G. J. *Rev. Sci. Instrum.* **1973**, *44*, 1.
(16) Walker, J. *Rep. Prog. Phys.* **1979**, *42*, 1605.

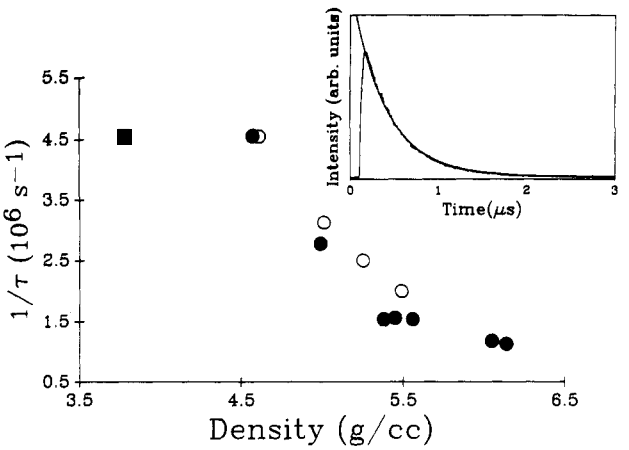

Figure 2. Density dependence of fluorescence decay rates: open circles, 298K data; filled circles, 30 K data; filled square is the decay rate of Xe_2Cl isolated in a zero pressure, 12 K xenon matrix. An example of the time evolution of fluorescence is shown in the inset, together with its single-exponential fit.

the observed lifetimes scale linearly with density; between the sample densities of 4.5–6.5 g cm^{-3}, the fluorescence lifetime increases from 220 to 1300 ns. As in the case of spectral shifts, in the first 3.0 GPa range, the lifetimes appear to be independent of pressure. At high pressures, the room temperature lifetimes are systematically shorter than those at 40 K.

While continuous excitation spectra proved difficult to obtain, due mainly to the broad featureless nature of the excitation band, emission was monitored at discrete wavelengths accessed with a dye laser. The main interest in these measurements was to determine the excitation threshold. The excitation threshold, under all studied conditions, was observed to overlap with the blue edge of the emission band. As an example, at 6.0 GPa pressure, and 30 K, the exciplexic emission could be observed for wavelengths as long as 590 nm. This is a rather dramatic effect, since in zero pressure solids a Stokes shift of nearly 0.5 eV is observed between the excitation and emission edges.[5]

The emission intensity, at pressures greater than 5.0 GPa, remains stable over the period of several weeks and shows a linear dependence on excitation intensity. The latter observation is essential to establish that the emission is due to the one-photon charge-transfer excitation between Cl atoms and Xe. The more striking conclusion is that, in the room temperature solid, as long as the pressure is kept above 5.0 GPa, the diffusion-controlled recombination of atoms proceeds on a time scale longer than several weeks. Upon depressuring the cell to 2.0 GPa, the emission intensity subsided over a period of ~3 h. A series of experiments, aimed at understanding the mechanisms of photodissociation of Cl_2 and recombination of Cl atoms, were conducted at this pressure and for temperatures ranging from 40 to 298 K. These are described next.

After complete recombination of atoms in the dark, irradiation of the sample at 308 nm regenerates the exciplexic emission. At ambient temperatures, the recombination and regeneration cycle is repeatable. Growth curves at low temperatures may be obtained by warming the sample, allowing for recombination, and then cooling and irradiating. At temperatures between 40 and 160 K, after an initial induction period, a temperature-dependent linear growth is observed. Examples of linear growth at several different temperatures are illustrated in Figure 3, and the initial induction period is shown in the inset to the figure. In the lower temperature range, the photogeneration quantum yields are small enough such that completion of the molecular dissociation is not a practical proposition. This is demonstrated in the inset to Figure 3 by a growth curve recorded at 120 K. This curve represents an irradiation period in excess of 10^5 laser pulses at a laser fluence of 10^{23} photons cm^{-2} s^{-1}. The initial induction period can also be seen in the inset to Figure 3. It should, however, be clear from Figure 3 that under the assumption of constant absorption cross section the temperature dependence of photogeneration quantum

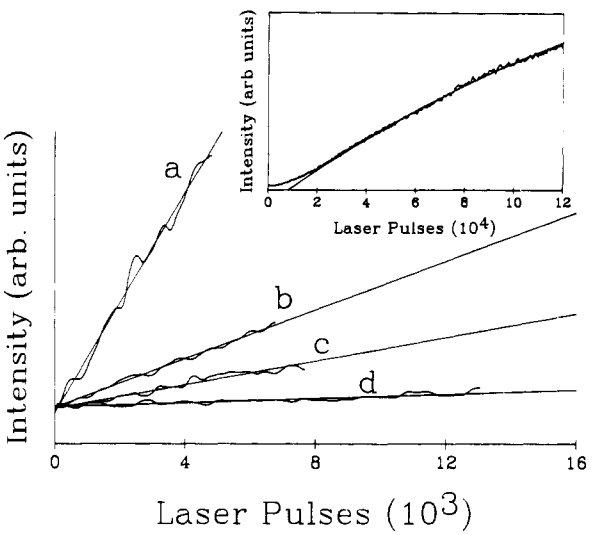

Figure 3. Growth curves in the DAC at 2.0 GPa. The linear portion of growth curves is illustrated: (a) 160 K, (b) 130 K, (c) 75 K, (d) 46 K. In the inset an extended growth curve at 120 K, which displays the early induction time, is shown along with a fit to a single exponential. In all cases the sample is irradiated with a pulsed XeCl laser at 308 nm, with a pulse width of 20 ns and fluence of 2×10^{16} photons cm^{-2}·$pulse^{-1}$.

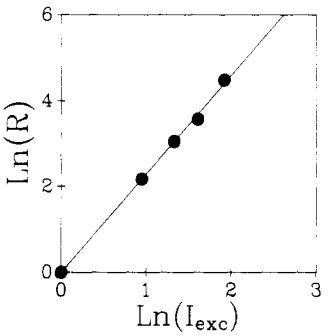

Figure 4. Power dependence of growth rates. A log–log plot of the rate (R) of fluorescence growth (slope of linear growth curves) versus irradiation fluence (I_{exc}) is shown. Both ordinates are in arbitrary units. A power dependence of 2.3 ± 0.3 is obtained from the linear fit.

yields can be extracted from the growth rates. The growth rates increase by a factor of ~50 in the range 40–160 K. Throughout this temperature range, the growth rate is found to have a second-order dependence on excitation fluence. This is illustrated in a log–log plot in Figure 4, for data obtained at 120 K, for nearly a decade in input energies; a power dependence of 2.3 ± 0.3 is obtained.

At temperatures above 120 K, depending on sample irradiation and temperature cycling history, a variety of growth behaviors is observed. These variations arise due to both temperature-induced and photoinduced diffusion and subsequent recombination of atoms. Temperature-induced recombination is demonstrated by first photogenerating the emission at 40 K and subsequently monitoring the emission during sample warm-up. An example is shown in Figure 5. In the illustrated case, the sample was heated at a rate of ~1.2 K min^{-1}, while data were collected at intervals of ~10 min. The curve is characteristic of an activated rate process: activated diffusion and subsequent recombination of atoms.[17] A crude estimate of the activation energy can be obtained from the inflection point of this sigmoidal curve as 230 K. It is also possible to clearly demonstrate photoinduced recombination in these solids. This is achieved by first photogenerating the atoms at low temperatures (at which a linear growth in emission intensity is observed), subsequently raising the sample temperature, and monitoring the decay of emission as a function

(17) Borg, R. J.; Dienes, G. J. *An Introduction Solid State Diffusion*; Academic Press: New York, 1988.

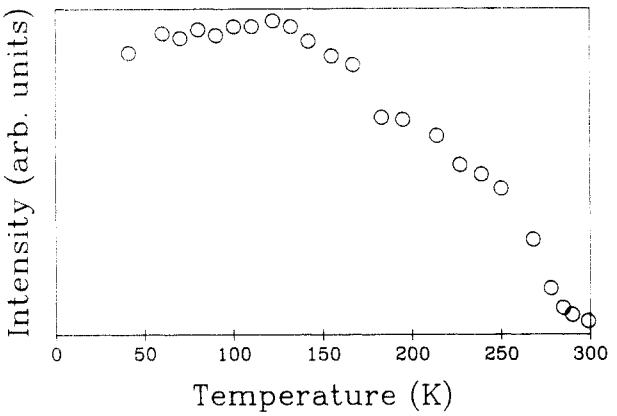

Figure 5. Thermal recombination of atoms. The decay of emission intensity as a function of temperature is shown. The data were obtained after extensive irradiation of the sample (2 GPa, 40 K), and during warm up. The cell temperature was raised at a rate of 1.2 K min^{-1} in the dark, and emission intensities were recorded by 308-nm excitation at 10-min intervals.

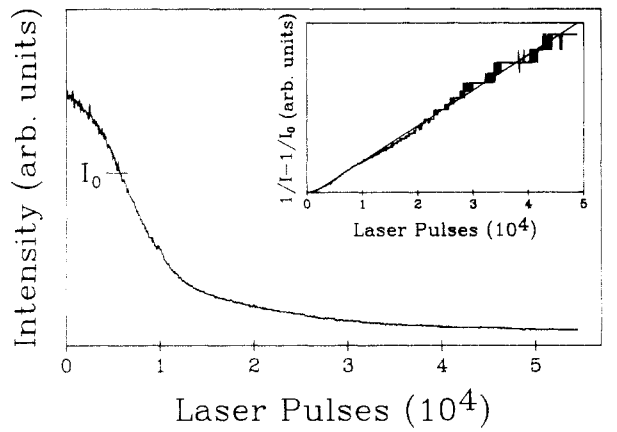

Figure 6. Photoinduced recombination of atoms. After extensive irradiation of the sample, the DAC temperature is raised to 160 K, and the emission intensity of Xe_2Cl is monitored continuously during irradiation. The irradiation source is a XeCl laser at 308 nm with pulse width of 20 ns and a fluence at 7×10^{15} photons cm^{-2} $pulse^{-1}$. After an initial induction period, the fluorescence decays hyperbolically. This is illustrated in the inset, by plotting the reciprocal of intensity versus number of irradiation pulses (or time). The portion of the decay belonging to the induction period, indicated by I_0, is ignored in the inset.

of irradiation time. Such a photoinduced decay curve is shown in Figure 6. The behavior is characterized by an initial induction period and a subsequent hyperbolic decay, the latter being characteristic of second-order processes. Ignoring the induction period, a linear dependence of the reciprocal intensity on irradiation time can clearly be obtained as illustrated in the inset to Figure 6. The latter part of this behavior can clearly be ascribed to photoinduced, diffusion-controlled atomic recombination. It is found that the temperature-induced recombination is strongly dependent on the sample temperature and irradiation history. Particularly, samples cycled and irradiated at higher temperatures (100–200 K) show little or no temperature-controlled diffusion at 160 K, while samples freshly irradiated at low temperatures (<100 K) exhibit the dark diffusion upon warm-up.

An example of a room temperature growth curve is illustrated in Figure 7. A plateau is reached in this case, however, at a limit much lower than those attained in the linear growth periods at lower temperatures. The room temperature growth fits the tanh form. After the plateau is reached, an increase in irradiation intensity produces renewed growth, and a higher plateau is reached. The tanh behavior at a given photon fluence is characteristic of first-order generation and second-order (i.e., diffusion controlled) recombination of atoms. The increase in the asymptotic limit of the growth with increasing photon fluence is consistent with photon dependencies of second order for dissociation and first

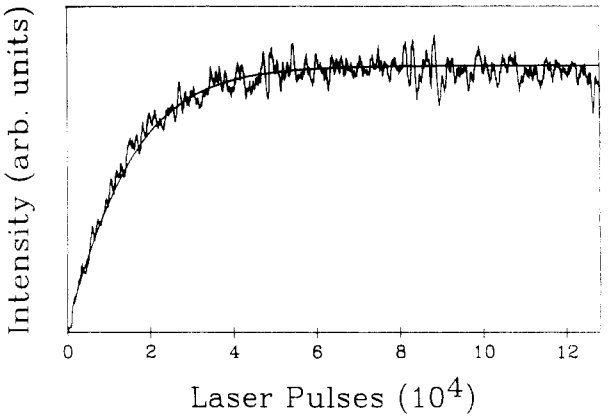

Figure 7. Room temperature growth curve. After complete recombination of atoms, the growth in the exciplex emission intensity is monitored while irradiating the sample at 308 nm (7×10^{15} photons cm^{-2} $pulse^{-1}$). The curve fits the tanh form, which is also shown.

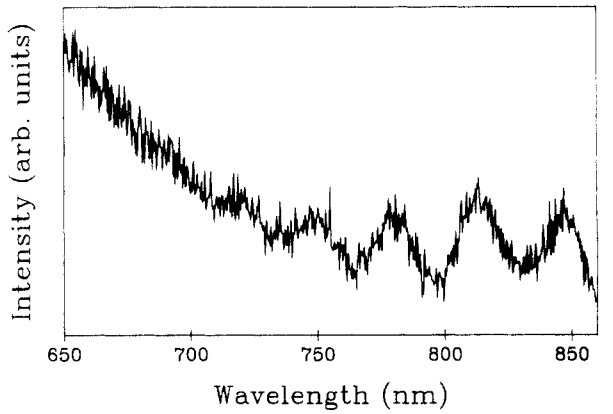

Figure 8. $Cl_2(A'\rightarrow X)$ emission spectrum from the DAC, at 2 GPa and 40 K. The molecular emission is seen as the tail of the exciplex emission, the blue edge is due to the cutoff of the PMT used.

order for recombination. For a detailed kinetic analysis see the Discussion section. The fact that, for a given excitation fluence, at higher temperatures lower asymptotic limits are reached implies that the photoinduced recombination process has a temperature dependence stronger than that of the photodissociation.

Finally, in order to test that we are monitoring the photodynamics of isolated Cl_2 molecules, an emission spectrum of the $Cl_2(A'\rightarrow X)$ transition was recorded. This is shown in Figure 8. This emission has been previously studied extensively. In solid xenon the lines are broad; however, in solid Cl_2 and in Cl_2 clusters, they completely merge resulting in a broad continuum type emission.[13] The observation of the vibrational progression, with valleys that reach the dark background, implies that we are indeed monitoring the dynamics of isolated molecules.

At the end of the 2.0 GPa studies, and ~6 months after the initial loading of the sample, the cell pressure was raised to 5.0 GPa. The growth of emission was monitored, and it was established that at room temperature no recombination occurs over extended periods. This is illustrated in Figure 9, in which emission spectra taken 20 days apart after photogeneration of atoms are shown. Using the diamond emission as an internal standard, it can clearly be seen that no dark recombination occurs for such periods of time at room temperature. Using the diamond fluorescence as reference, it was established that emission intensity in this case was an order of magnitude lower than those obtained in the freshly loaded sample (see Figure 1a). Whether this difference is entirely due to loss of chlorine, due to diffusion out of the field of view, could not be firmly established since even after irradiation with 10^5 pulses at a fluence 10^{16} photons cm^{-2} s^{-1}, the growth in emission was not complete. This discrepancy introduces a significant uncertainty in the quantitative analysis of the data, since absolute number densities are required for the extraction

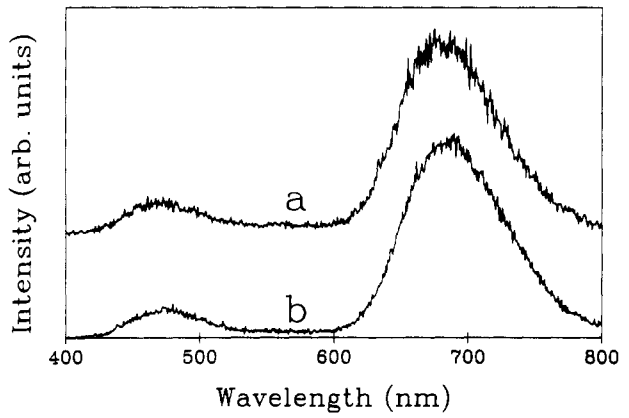

Figure 9. Absence of recombination at 5 GPa. Room temperature emission spectra from the DAC taken 20 days apart are shown. The relative intensities of the Xe_2Cl emission (near 700 nm) and the diamond fluorescence (near 470 nm) are within experimental error identical, implying the absence of any atomic recombination.

of second-order rate constants. Completion of dissociation in the initial studies is a safe assumption, since most of the irradiation was carried out at cryogenic temperatures and at zero pressure.

Discussion

Spectroscopy. The charge-transfer states of solid xenon doped with atomic halogens have previously been studied extensively in matrices.[5] The only emission in such solids is attributed to the triatomic exciplex, Xe_2Cl in this case. The parentage of this species has been directly established by following the emission in gas, supercritical fluid, liquid, and solid phases.[18,19] Strong evidence for the clustering of the exciplex in both the gas and liquid phase has been presented previously.[18,20] While the main effect of density is a large red shift in emission due to solvation of the ionic excited state, an interesting effect of clustering is that upon liquid–solid phase transitions an abrupt blue shift is observed.[20,21] The latter effect is most clearly observed in the case of Xe_2I/Xe solutions, which upon slow freezing yield single crystals. The blue shift has been attributed to dilation of the first cluster shell upon crystallization.[21] The similarity of emission profiles under high pressure to that of the zero pressure, the linear shift of the emission maximum, and the linear decrease of fluorescence lifetimes all serve the identification of the emitter from the cell as Xe_2Cl isolated in solid xenon. Given the large dipole of the upper ionic state (~12 D for the isolated exciplex), a large shift of this emission with density, as observed for densities greater than 5 g cm^{-3} in Figure 1b, is to be expected. It is then interesting to speculate on the origin of the observed initial density independence of the shift (see Figure 1b). Given the short range of dipole–induced dipole interactions, the main contribution to spectral shifts is expected to be from the immediate neighbors of the exciplex. Given the very large magnitude of dipole of this upper state, it should also be expected that in the zero pressure solids, upon creation of the ionic state, a compression of the immediate isolation cage occurs. A spectral shift as a function of external pressure would then only be observed if the bulk density exceeds the zero-pressure local density around the exciplex. From Figure 1b, according to this hypothesis, it can be deduced that the local density at zero pressure is nearly 30% higher than the bulk density of 3.8 g cm^{-3}.

The observed density dependence of lifetime elongation (Figure 2), is rather similar to that of the lineshift (Figure 1b) and therefore suspected to have the same origin. We first note that the effect of simply increasing the density of the medium, hence increasing the bulk dielectric, would be one of lifetime shortening.[22] However, given the very large red shift of the transition, and under the assumption of constant oscillator strength, f, a lifetime elongation may be expected (since $f\tau \propto \lambda^2$). While this consideration qualitatively accounts for the observed correlation between lifetime and lineshift, it fails on a quantitative level. A nearly 6-fold increase in lifetimes is observed in the studied range of densities, while on the basis of the constant oscillator strength assumption only a factor of 1.6 is to be expected from the spectral shift. Clearly a reduction in transition dipoles accompanies the increase in density. A partial delocalization of charge could in principle explain this behavior. Finally, it is worth noting that, while the fluorescence lifetime is somewhat reduced in going from 40 to 300 K, the deactivation remains mostly radiative. This is not too surprising given the fact that it had previously been demonstrated that even in the presence of translational degrees of freedom, in room temperature supercritical fluid Xe, Xe_2Cl relaxes radiatively.[18]

The fate of the vertically accessed charge-transfer states of rare gas solids doped with atomic halogens under high pressures is in itself a very intriguing subject. It has previously been shown that in Cl-doped xenon, at zero pressure, the vertically accessed charge-transfer states are extensively delocalized[5] and yield themselves to a description in terms of a Rydberg hole progression.[23] The effect of increased density on these states should be significant. Both the increase in the valence bandwidth of the solid and the increase in the dielectric of the medium as the gap is narrowed would promote hole delocalization. As such it would be expected that the Wannier type excitonic description becomes even more appropriate, and therefore large-orbit Rydberg states can both be accessed optically and sustained with longer lifetimes. The spectroscopic characterization of these states has not yet been completed. Studies to date indicate that the excitation band is broad and structureless and has extended to the blue edge of the emission band. In order to observe the Rydberg progressions, it is essential to carry out studies at very low temperatures to minimize spectral broadening due to the coupling of these extended states to lattice phonons. For the present report, we note that the exciplexic emission can be induced in a very broad spectral range, and the dramatic shift in excitation threshold at even 6.0 GPa (a shift of 1.5 eV relative to zero pressure) implies that at least in some trapping sites the triatomic states are directly accessible. This could imply that, under high-pressure conditions, trapping and stabilization in T_d sites is possible (at zero pressure, halogen atoms are found only in O_h and substitutional sites).

Two main conclusions that are crucial for the exposition of the rest of this discussion are to be drawn from the above. First, the emission spectra probe the charge-transfer transitions of Cl/Xe, and therefore emission intensities can be directly used as a measure of number densities of Cl atoms in the solid. The second important conclusion is that, since the line shape of this bound to repulsive transition is not effected by pressure, the radiative dissociation of the triatomic leads to the same location on the repulsive surface of the ground potential. We may therefore rely on the previous solid-state spectral analysis of this emission to conclude that, upon radiation, the system is born ~1 eV above ground, with initial impulses equally partitioned along the Xe–Xe and Xe_2–Cl coordinates.[4] The radiative dissociation of the exciplex therefore leads to the creation of hot atoms which may migrate in the lattice. This is the origin of photomobility, which is observed in these systems, and which will be further amplified below.

Dark Diffusion. The first set of important conclusions pertain to atomic diffusion. The absence of any recombination at pressures above 5.0 GPa for periods of weeks implies a very low mobility of the trapped radical atoms. If we assume that the dissociation was complete under these conditions, a reasonable assumption since no further growth could be observed with extensive irradiation, then a diffusion constant can be derived as

(18) Okada, F.; Apkarian, V. A. *J. Chem. Phys.*, in press.
(19) Wiedeman, L.; Fajardo, M. E.; Apkarian, V. A. *J. Phys. Chem.* **1988**, *92*, 342.
(20) Okada, F.; Wiedeman, L.; Apkarian, V. A. *J. Phys. Chem.* **1989**, *93*, 1267.
(21) Lawrence, W.; Okada, F.; Apkarian, V. A. *Chem. Phys. Lett.* **1988**, *150*, 339.
(22) See for example: Fulton, R. L. *J. Chem. Phys.* **1974**, *61*, 4141.
(23) Schwentner, N.; Fajardo, M. E.; Apkarian, V. A. *Chem. Phys. Lett.* **1989**, *154*, 237.

$$D \lesssim \frac{1}{4\pi n r t_{1/2}} = 2 \times 10^{-20}\ \mathrm{cm^2\ s^{-1}}$$

in which $t_{1/2}$ is the time scale for 50% recombination taken to be longer than 1 week, n is the Cl atom number density assuming a Cl:Xe ratio of 1:250, and r is the radius of contact at which recombination occurs, taken to be 4 Å. The implication of this very small diffusion constant (nearly 10 orders of magnitude less than diffusion constants near the melting point of solids) is that, at pressures in excess of 5.0 GPa, Cl atom number densities of 1:250 are essentially immobile in room temperature xenon!

The observation of a half-life of ~3 h for recombination at 2.0 GPa, and for an initial Cl atom number density of 1:2500 (as estimated from the exciplex/diamond relative emission intensities), implies a diffusion constant of $\sim 2 \times 10^{-17}$ cm^2 s^{-1} at room temperature. As a point of calibration, we note that this diffusion constant is similar in value to that of atomic self-diffusion in metals.[24] Under proper annealing conditions, at 160 K and 2.0 GPa of pressure, the photogenerated atom density remains stable overnight. It can therefore be concluded that, for nearly a factor of 2 reduction in temperature, the diffusion constant of Cl atoms is reduced by more than an order of magnitude. This would imply an activation energy for diffusion in excess of 800 K. This is to be contrasted with the observation that in freshly irradiated solids (see Figure 5) an activation energy of 230 K is obtained during the warm-up cycle. With these two examples, we illustrate the experimental finding that *thermally induced recombination is a strong function of the prior history of the solid.* In addition to the irradiation, and annealing history of the solids, a very strong dependence of diffusion constants on pressure is observed. The latter is as a general rule to be expected for compressible solids. However, the nearly 3 orders of magnitude reduction in diffusion constants upon tripling of pressure is an impressive effect. The very strong dependences of diffusion constants on density and sample history are clear indications that a vacancy-mediated mechanism is operative. Direct evidence to this effect is obtained from the observed induction periods in photogeneration and photoinduced mobilities, as will be discussed below. It is important to note that, if diffusion is vacancy mediated, its quantitative determination is sensitive to the density of imperfections in the solid. In the absence of a direct measure of defect concentrations, the diffusion constants derived above should be regarded as upper limits for the true values, i.e., for the diffusion constants in the perfectly annealed crystal.

Photoinduced Mobility. A clear demonstration of photoinduced mobility of Cl atoms and subsequent diffusion-controlled recombination is given in Figure 6. The experimental procedure in obtaining these data was similar to that used in the demonstration of dark thermal diffusion in Figure 5. As such it does not represent data from a well-annealed system. We will therefore refrain from quantitative analysis and suffice by the insights implied from the observed time evolution of recombination during sample irradiation. The origin of photomobility upon radiative dissociation of exciplexes is well understood and has recently been documented in some detail in studies of fluorine-doped solid Ar and Kr.[25] Upon the radiative dissociation of the triatomic exciplex, the ground covalent potentials are accessed on the repulsive wall ~1 eV above ground. Moreover, relative to nearest-neighbor distances in solid Xe, the Xe–Xe distance in the suddenly created pair is shorter by more than 1 Å. This sudden release of repulsive energy cannot be directly accommodated by the lattice. As a result, shock waves, local defects, and atomic mobility are observed.[25] As indicated by the hyperbolic decay of the emission intensity in the inset to Figure 6, after an initial induction period the Cl atoms recombine by diffusion. This would imply cage exit and execution of a random walk through the lattice upon radiative dissociation. The induction period would then suggest that initially the hot atoms are not able to execute any mobility: they are trapped near their original sites of isolation. The impulsive energy released in this period evidently facilitates the final mobility, presumably by the creation of lattice defects. We take this observation as a direct indication that atomic mobility and diffusion are defect, or equivalently vacancy, mediated.

Photodissociation. The similarity of photodissociation and radiative dissociation in solids is one that has been well appreciated previously.[25] In both cases atomic fragments are created with excess energy, and success is measured by the probability of cage exit of fragments. It is, therefore, not surprising that as in the case of photomobility an induction time is seen in the photogeneration process as well (inset to Figure 3). After the initial induction period, a growth in fluorescence (or equivalently in atomic concentrations) linear with irradiation time is observed. This was illustrated in Figure 3. Since completion of photogeneration is not achieved, absolute cross sections cannot be extracted from the data without intensity calibration. However, relative cross sections and, in principle, relative quantum yields can be extracted without making any assumptions. A strong temperature dependence of quantum yields, an increase by a factor of 50 in the range 40–160 K, is directly obtained from the slopes of the linear growth curves. As will be discussed below, a further increase by 2 orders of magnitude in growth rates is observed between 160 and 300 K. Thus the efficiency of the photogeneration of atoms, at 2 GPa, increases by nearly 3 orders of magnitude between 40 K and room temperature in this system.

The observation of two-photon dependence for the photogeneration of atoms at all studied pressures, temperatures, and irradiation fluences clearly indicates that in this case, as in cryogenic Xe matrices, the operative mechanism is the two-photon-induced harpoon process:[4]

$$Cl_2 + Xe + 2h\nu \rightarrow [Xe^2Cl_2^-] \rightarrow Xe^+Cl^- + Cl \qquad (1)$$

The Cl atom photogeneration cross section (i.e., the product of two-photon charge-transfer excitation cross section, σ_2, and cage exit quantum yield, ϕ_2, by the mechanism of eq 1) has been extracted from growth curves in Xe matrices[4] as $\phi_2\sigma_2 = 10^{-43}$ cm^4 s. Transmission measurements in liquid Xe[13] have yielded a value for $\phi_2\sigma_2$ at 308 nm of 6×10^{-45} cm^4 s. The solid-state cross sections are subject to larger errors since they are extracted from kinetic analysis of growth curves which involve several parameters. Although an increase in charge-transfer excitation cross sections is to be expected in the denser media, the liquid-phase cross section is thought to be more reliable since it involves a more direct measurement—transmission as a function of input power. Given the fact that the DAC sample remains optically thin throughout the irradiation period, at low temperatures, at which neither dark diffusion nor photomobility is significant, a simple exponential growth of Cl atom concentrations is to be expected on the basis of eq 1

$$[Cl] = 2[Cl_2]_0[1 - \exp(-I^2\sigma_2\phi_2 n\Delta t)] \qquad (2)$$

in which [Cl] is the time-dependent Cl atom concentration, $[Cl_2]_0$ is the initial Cl_2 concentration, I is the irradiation fluence per pulse in units of photons cm^{-2} s^{-1}, σ_2 and ϕ_2 are the two-photon cross-sections and quantum yield of cage exit, respectively, Δt is the laser pulse width of 20 ns, and n is the number of deposited laser pulses. Although incomplete even after 10^5 pulses, the 120 K growth curve illustrated in the inset to Figure 3 shows sufficient curvature to enable at least an estimate by fitting it to the exponential rise form of eq 2. A two-photon cross section for generation of atoms $\sigma_2\phi_2 = 4 \times 10^{-47}$ cm^4 s is obtained from the fit, much smaller than either Xe matrix or liquid Xe cross sections. The contributions to the reduction in this cross section in the 2 GPa solid from excitation cross section, σ_2, and the cage exit quantum yield, ϕ_2, cannot be separated with the available data. Both are expected to decrease as a function of pressure. A reduction in ϕ_2 is to be expected, since charge-transfer transitions undergo large red shifts with density and the present excitation wavelength (308 nm) is already to the blue of the two-photon-excitation maximum of 340 nm observed in liquid Xe.[13]

(24) Smithells. In *Metal Reference Book*, 6th ed.; Braudes, E. A., Ed.; Butterworth, 1983; Section 13.10.

(25) Kunttu, H.; Feld, J.; Alimi, R.; Becker, A.; Apkarian, V. A. *J. Chem. Phys.* **1990**, *92*, 4856.

The estimate of the two-photon-induced dissociation cross section serves to establish an upper limit on the direct dissociation of Cl_2 via its one-photon $^1\Pi_u \leftarrow X$ dissociative absorption:

$$Cl_2(X) + h\nu \rightarrow Cl_2(^1\Pi_u) \rightarrow Cl + Cl \quad (3)$$

This mechanism is the standard dissociation channel, and the one considered by the MD simulations, which motivated these studies.[8] A search for one-photon dissociation, by reduction of the irradiation fluence to the lowest limits of growth rate detectivity, proved fruitless. It can therefore be inferred that the quantum yield of this direct dissociation channel is very small, given by

$$\phi_1 < \phi_2\sigma_2 I/\sigma_1 \quad (4)$$

in which the subscripts 1 and 2 refer to the one-photon and two-photon photogeneration processes of eqs 3 and 1, respectively. With the assumption that the absorption cross section of molecular Cl_2 ($\sigma_1 = 1.9 \times 10^{-19}$ cm^2 at 308 nm) is not affected in this pressure range, it can be established from eq 4 that the photodissociation quantum yield of Cl_2 in the 2 GPa solid is less than 10^{-6} at 40 K, and less than 10^{-4} at 160 K. Our experimental results are then in serious disagreement with the MD simulations which predicted a quantum yield of near unity in 160 K Xe. The discrepancy of nearly 4 orders of magnitude in quantum yields between experiment and theory cannot be ascribed to the only assumption made in this derivation, namely to the assumption that the molecular absorption cross section of Cl_2 is not altered. The comparison is, however, unfair, since the experiments are conducted at 2 GPa, while the simulations were limited to zero pressure. It would be rather interesting to test theoretically whether such a large effect can be induced by a change in density of 20%.

The time evolution of growth curves at temperatures above 160 K requires a kinetic analysis that includes photoinduced recombination processes. The kinetic model used for this treatment consists of the following minimal set of equations

(a) two-photon-induced harpoon process of eq 1 can be summarized as:

$$Cl_2 + 2h\nu \rightarrow Cl + Cl, \quad \phi_2\sigma_2 \quad (5)$$

(b) one-photon-induced creation of mobile Cl atoms, designated by Cl*:

$$Cl/Xe + h\nu \rightarrow Cl^*/Xe, \quad \sigma \quad (6)$$

(c) recombination upon encounter between mobile and stationary Cl atoms:

$$Cl^* + Cl \rightarrow Cl_2, \quad k \quad (7)$$

in which σ is the absorption cross section at 308 nm of the Cl/Xe charge-transfer excitation, and the detailed mechanism underlying eq 6 is the creation of kinetically hot Cl atoms by the radiative dissociation of Xe_2Cl. Recombination is then assumed to be due to diffusion-controlled encounters of the mobile atom with stationary Cl atoms, an approximation that can be well justified given the weak excitation fluences at which less than 0.1% of the Cl atoms are excited. The rate expression for this mechanism

$$\frac{d}{dt}[Cl] = 2I^2\sigma_2\phi_2[Cl_2]_0 - I^2\sigma_2\phi_2[Cl] - I\sigma\phi\Delta t[Cl]^2 \quad (8)$$

can be integrated to yield

$$[Cl] = \beta \tanh(1/\tau - \gamma) - \epsilon \quad (9)$$

with the definitions

$$K = I\sigma k\Delta t$$

$$z = [8I^2\sigma_2\phi_2K[Cl_2]_0 + I^4\sigma_2^2\varphi_2^2]^{1/2} \quad (10)$$

the parameters of eq 9 are given as

$$\beta = z/2K$$

$$\frac{1}{\tau} = \frac{z}{2}$$

$$\gamma = \tanh^{-1}\left[\frac{I^2\sigma_2\phi_2}{2K}\right]$$

$$\epsilon = \frac{I^2\sigma_2\phi_2}{2K} \quad (11)$$

in which I is the laser fluence in units of photons cm^{-2} s^{-1} and Δt = 20 ns is the laser pulse width. The asymptotic limit for Cl atom concentrations is then given as

$$[Cl]_\infty = \frac{z - I^2\sigma_2\phi_2}{2K} \quad (12)$$

which is a function of laser fluence. A fit to the growth curve with this form is presented in Figure 7. Two quantities are obtained from the fit without any assumptions and without an absolute calibration of the emission intensity. These are given in eqs 13 and 14

(a) the two-photon-dissociation cross section: $\sigma_2\phi_2 = \frac{2\epsilon}{I^2\tau\beta}$ (13)

for which a value of $\sigma_2\phi_2 = 1 \times 10^{-44}$ cm^4 s is obtained. This cross section is nearly 2 orders of magnitude larger than the 160 K value derived above, and very similar to the two-photon-excitation cross section derived in liquid Xe for this same process.[13] This would imply that the cage exit quantum yield, ϕ_2, in the room temperature solid is of order unity as in the case of liquid xenon.

(b) the fraction of Cl_2 dissociated: $\gamma = \frac{2\epsilon(\beta - \epsilon)}{\beta^2 - \epsilon^2} = 0.4$ (14)

under the irradiation conditions of the example shown in Figure 7. Here $[Cl] = 2\gamma[Cl_2]_0$ and $[Cl_2] = (1 - \gamma)[Cl_2]_0$ at photochemical equilibrium represented by the plateau of Figure 7. Note that this equilibrium is developed by the competition between two-photon-induced generation, and one-photon-induced recombination of atoms. As such, according to eq 12, when the excitation energy is increased, an increase in the final plateau, and hence fraction of dissociation, should be observed. This behavior is indeed observed, in good agreement with the model prediction.

In order to extract quantitative information about the extent of photomobility and diffusion of hot atoms in the solid, two inputs are necessary: the absolute concentration of chlorine in the sample, and the one-photon charge-transfer absorption cross section, σ, of eq 6. Neither of these is directly measured in the experiments. It is nevertheless useful to make estimates, in order to comment on the extent of photomobility in the room temperature solid. Comparison of the spectra shown in Figures 1 and 9, which were taken nearly 6 months apart, shows a factor of 20 reduction with time in the Xe_2Cl/diamond emission ratios. The implication is that, during the course of these studies, chlorine is lost from view in the cell. Diffusion of atoms and their subsequent reaction with the inconel gasket is a possible loss mechanism. If we then assume that the early spectra are representative of the originally loaded concentration, a Cl_2:Xe ratio of 1:5000 can be estimated for the later concentrations, i.e., a Cl_2 number density of 2×10^{19} cm^{-3}. Since at this number density only ~50% of the molecules can be dissociated, the photoexcited atoms would have to have a migration range λ given by the statistical separation between isolation sites of ~35 Å. If we assume that the estimate $\sigma = 1 \times 10^{-18}$ cm^2 obtained from matrix measurements is valid,[4] it is possible to extract a recombination constant, k, for eq 7 of 5×10^{-15} cm^3 s^{-1}. With the assumption that recombination is diffusion controlled, i.e., due to the random walk of the photoexcited "hot" atom, a diffusion constant $D = k/4\pi r \sim 10^{-8}$ cm^2 s^{-1} can be obtained (using r = 3 Å for the recombination radius). Both of

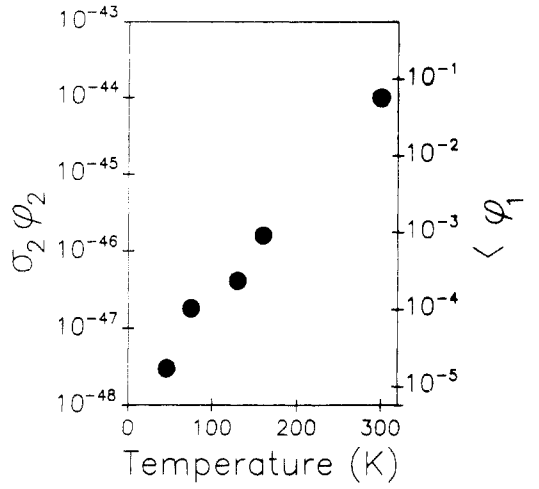

Figure 10. Temperature dependence of photogeneration probabilities. On the left ordinate the two-photon-induced photogeneration cross section, $\phi_2\sigma_2$, is presented, while on the right ordinate the upper limit for quantum yields of direct photodissociation, ϕ_1, is presented ($\phi_1 < \phi_2\sigma_2 I/\sigma_1$, see text).

these estimates, λ and D, for the hot atoms are extremely large in view of the packing density of the solid and the dark diffusion constants discussed earlier. The only possible rationalization is that the recombination proceeds via long-range migration of atoms upon the initial impulse, a mechanism observed both theoretically[26] and experimentally[25] for F atoms in cryogenic Ar.

Conclusions

With this paper we demonstrate that photodynamical studies, dissociation diffusion and recombination measurements, can conveniently be accomplished under high pressures by the use of diamond anvil cells. The extended temperature and density scales provided by this technique are extremely useful for accurate characterizations of many-body dynamics in van der Waals solids and enable rigorous comparisons between experiment and theory. The present results should encourage theoretical investigations with the solid density as a real variable. It is experimentally possible for example to compress Xe to reach the lattice constant of zero-pressure Kr. The equivalent exercise is somewhat simpler to achieve in computer simulations. Such combined efforts could scrutinize the effects of mass, potentials, and packing densities on a given dynamical process, and should therefore become instrumental in developing a general understanding of condensed-phase dynamics.

The system chosen for the present studies, Cl_2 in solid Xe, was in part motivated by recent MD simulations of photodissociation dynamics of the same. The temperature dependence of cage exit quantum yields is one observable that serves as testing grounds between experiment and theory. As such, we summarize the temperature dependence of photogeneration cross sections measured, and the implied upper limits for quantum yields of direct molecular dissociation in Figure 10. The theoretical predictions for Cl_2 dissociation in zero-pressure Xe are 0.1 at 90 K and 0.3 at 160 K. The nearly 5 orders of magnitude difference between our results and the theoretical predictions could in principle be ascribed to the difference in pressure between the two. If so, a very strong pressure dependence is being observed which would be interesting to test in theoretical simulations.

While direct photodissociation of Cl_2 in Xe is prohibited by a strong cage effect even at room temperature, two-photon-induced dissociation via ionic potentials maintains a large cross section. At room temperature, the cross section of this process is only a factor of 2 smaller in 2 GPa solid Xe than the two-photon charge-transfer absorption cross section of the same process previously measured in liquid Xe. Making the reasonable assumption that excitation cross sections are similar in the two media, it would follow that quantum yields of cage exit by the photoinduced harpoon process is near 0.5. The cross section for dissociation via this process shows a strong temperature dependence—3 orders of magnitude reduction between room temperature and 40 K. This decrease should mainly be interpreted as due to the reduction in quantum yields, i.e., reduction in cage exit probabilities.

The photodynamics of radiative dissociation of exciplexes in solids can be as insightful as photodissociation. In the case of Xe_2Cl, we show that upon radiative dissociation the Cl atoms undergo extensive migration. The extracted diffusion constant and migration range of the Cl atoms by this process are too large to be explained by atomic diffusion in intact crystals. Directed long-range migration is hypothesized. This process is triggered by the sudden release of $\sim$1 eV of kinetic energy, initially equally partitioned among the Xe–Xe and Xe_2–Cl coordinate. Such an excess energy cannot be accommodated by the atomic lattice. The modes of degradation of this energy into the phonon bath and its dependence on the initial impulse characteristics are the subjects of recent studies of fluorine-doped solid Kr and Ar.[24] In addition to atomic mobility, ballistic and diffusive shock waves have been identified in those studies. Under high pressures, the sudden creation of shock waves internally could have interesting effects on chemical dynamics and reactivity. The possibility that long-range migration is induced by such effects cannot be discarded.

We have characterized the dramatic effect pressure plays on diffusion constants of impurities trapped in a solid. This observation, which should be of general applicability to all compressible solids, is perhaps not too surprising. Yet it is impressive to isolate radicals at densities of 10^{20} cm^{-3}, in a room temperature sample, and to maintain them without any detectable recombination for periods of several weeks. In addition to the strong pressure dependence of diffusion constants, a strong temperature dependence is also observed. That dark diffusion, and photoinduced mobility, are both mediated by defects was directly demonstrated by the observation of induction periods and a strong dependence of diffusion constants and effective activation energies on the sample history.

Finally, we point out that charge-transfer transitions of rare gas–halogen atom systems is useful as a laser-induced fluorescence technique for photodissociation studies. The sensitivity of the technique in the present studies could be demonstrated by monitoring atom densities less than 10^{17} cm^{-3} in a total volume of 10^{-6} cm^3. The characterization of these charge-transfer transitions, and the dynamics that follows, are themselves major goals in these studies. Data presented on the density dependence of emission profiles and lifetimes led to the conclusion that, while the lowest energy charge-transfer complex in the system remains the molecular triatomic exciplex, some charge delocalization does occur at pressures in excess of 3 GPa. Further spectroscopic analysis, in particular of the excitation spectra in these solids, is necessary to develop a firmer understanding of hole transport energetics and dynamics which has previously been investigated in zero-pressure matrices.

Note Added in Proof. During the six month period after submission of this manuscript, the DAC containing atomic Cl in Xe was maintained at 5 GPa. Irradiation of the cell at 308 nm yielded a clearly visible emission near 700 nm, due to Xe_2Cl (see Figure 9). We conclude that at pressures above 5 GPa there is no detectable recombination of Cl atoms in atomic Xe.

Acknowledgment. This work was supported by the U.S. Air Force Astronautics Laboratory under Contract Fo4611-87-K-0024. The very useful discussions with Professor Malcolm Nicol, at the onset of this project, are gratefully acknowledged.

(26) Alimi, R.; Gerber, R. B.; Apkarian, V. A. *J. Chem. Phys.* **1990**, *92*, 3551.